AD-787 873

S/P TRAVEL TIME RATIO IN CENTRAL ASIA

Jack G. Swanson

Teledyne Geotech

Prepared for:

Air Force Office of Scientific Research
Advanced Research Projects Agency

September 1974

UNCLASSIFIED

SECURITY CLASSIFICATION OF THIS PAGE (When Data Entered)

REPORT DOCUMENTATION PAGE		READ INSTRUCTIONS BEFORE COMPLETING FORM
1. REPORT NUMBER AFOSR - TR - 74 - 1662.	2. GOVT ACCESSION NO.	3. RECIPIENT'S CATALOG NUMBER AD 787873
4. TITLE (and Subtitle) S/P Travel Time Ratio in Central Asia		5. TYPE OF REPORT & PERIOD COVERED Semiannual Period Ending 31 March 1974
		6. PERFORMING ORG. REPORT NUMBER TR 74-9
7. AUTHOR(s) Jack G. Swanson		8. CONTRACT OR GRANT NUMBER(s) F44620-74-C-0021
9. PERFORMING ORGANIZATION NAME AND ADDRESS Teledyne Industries, Inc., Geotech Division 3401 Shiloh Road, Garland, Texas 75041		10. PROGRAM ELEMENT, PROJECT, TASK AREA & WORK UNIT NUMBERS 62701E AO 1812-22
11. CONTROLLING OFFICE NAME AND ADDRESS Advanced Research Projects Agency/NMR 1400 Wilson Blvd., Arlington, Virginia 22209		12. REPORT DATE September 1974
		13. NUMBER OF PAGES 30
14. MONITORING AGENCY NAME & ADDRESS(if different from Controlling Office) Air Force Office of Scientific Research/NPG 1400 Wilson Blvd. Arlington, Virginia 22209		15. SECURITY CLASS. (of this report) Unclassified
		15a. DECLASSIFICATION/DOWNGRADING SCHEDULE

16. DISTRIBUTION STATEMENT (of this Report)

Approved for public release; distribution unlimited.

17. DISTRIBUTION STATEMENT (of the abstract entered in Block 20, if different from Report)

18. SUPPLEMENTARY NOTES

19. KEY WORDS (Continue on reverse side if necessary and identify by block number)

S/P Travel Times
Depth of Focus
Central Asia

20. ABSTRACT (Continue on reverse side if necessary and identify by block number)

The S/P travel time ratio for intermediate depth Hindu-Kush earthquakes is investigated, using S and P arrival times at 6 World Wide Standard Seismograph Network stations and 19 other close-in stations. Station mean values of the ratio range from 1.74 to 1.81, with an overall mean value of 1.78. The S/P travel time ratio increases slowly with increasing distance over the distance range 4.5 to 13.0 degrees, and increases rapidly with decreasing distance for distances less than 4.5 degrees. Variation of the ratio

DD FORM 1 JAN 73 1473 EDITION OF 1 NOV 65 IS OBSOLETE

UNCLASSIFIED

SECURITY CLASSIFICATION OF THIS PAGE (When Data Entered)

20. ABSTRACT (continued)

with focal depth is weak. The standard deviationof S/P origin time deviations from origin times based on locations restrained to pP depth is about 1.0 second, implying a standard deviation of S/P depth error, relative to pP depth, of 10 to 12 km.

CONTENTS

ILLUSTRATIONS

TABLES

S/P TRAVEL TIME RATIO IN CENTRAL ASIA

1. INTRODUCTION

This report describes work accomplished from October 1, 1973, through 31 March 1974, on the investigation of the use of close-in P and S arrivals to determine focal depth of seismic events in Central Asia. Emphasis of the study to date has been on empirical calibration of the S/P travel time ratio for earthquakes in or near the Hindu-Kush intermediate depth source observed at stations within 13 degrees of the source. The report includes an evaluation of the importance of depth and distance dependence of the S/P travel time ratio.

The S/P travel time ratio for shallow Central Asia earthquakes observed at close-in stations is currently being investigated.

In section 2 the basic background required to understand the theory behind the method used is briefly discussed. The use of P and S velocities on depth of focus and origin time determinations is emphasized together with the calibration of close-in stations and the use of Wadati graphs (Wadati, 1933, Kisslinger and Engdahl, 1973). In sections 3 and 4 the data used in the study and the methods employed are described. In section 5 the results obtained are discussed.

2. BACKGROUND

The modified Geiger method (Macelwane and Sohon, 1932) commonly used to locate earthquakes yields more accurate focal depth if origin time is known independently of the P arrival times used to make the location (Evernden, 1969, Swanson, 1969, 1971, Kisslinger and Engdahl, 1973). Origin time (T_S) can be computed from S and P arrival times at a single station if the ratio of S to P travel times is known for the path from hypocenter to station:

$$T_S = P - (S-P)/r \qquad (1)$$

where $r \equiv (\tau_s/\tau_p) - 1$

$\tau_s \equiv$ S travel time

$\tau_p \equiv$ P travel time

$S \equiv$ S arrival time

$P \equiv$ P arrival time

$T_S \equiv$ origin time estimated by the S/P technique

Depth (h_s) is then estimated by a routine location procedure with origin time restrained to T_s. The depth accuracy to expect when locating with the modified Geiger technique with origin time restrained may be clarified by the theory of hypocenter control factors (Veith and van Leer, 1970). The depth control factor for a given station is defined as the change in depth estimate resulting from a 1 second residual at the station. For the ideal case of a symmetrical net, so there is no interaction between epicenter and depth estimates, the depth control factor for station i is given by

$$\text{(depth control factor)}_i = \frac{(\partial t/\partial h)_i}{\sum_i (\partial t/\partial h)_i^2}$$

The change in depth (dh) is given by

$$dh = \frac{\sum_i (\partial t/\partial h)_i u_i}{\sum_i (\partial t/\partial h)_i^2}$$

where $u_i \equiv$ travel time residual at station i

If origin time is restrained to an erro eous value ($T' = T + \delta T$), then

$$dh' = \frac{\sum_i (\partial t/\partial h)_i \ (u_i - \delta T)}{\sum_i (\partial t/\partial h)_i^2}$$

or

$$dh' = dh + \frac{\sum_i (\partial t/\partial h)_i}{\sum_i (\partial t \ \partial h)_i^2} (-\delta T)$$

Therefore, the error in depth (δh) resulting from an error in origin time (δT) is given by

$$\delta h = \frac{\sum_i (\partial t/\partial h)_i}{\sum_i (\partial t/\partial h)_i^2} (-\delta T)$$

As a rule of thumb, for a good net of stations (Swanson, 1969):

$$\delta h \approx \frac{-\delta T}{(\partial t/\partial h)_{\bar{\Delta},h}}$$

where $\bar{\Delta} \equiv$ mean distance of locating net.

The accuracy with which r (see equation 1) must be known for a specified accuracy in T_s may be estimated easily, assuming no arrival time errors in S or P:

$$\delta r \approx \frac{r^2}{(S-P)} \delta T$$

where $\delta T \equiv$ origin time error

$\delta r \equiv$ error in r

For example, assuming a value of 0.78 for r and an S-P time of 25 seconds, an error in r of .024, or one part in 33, will result in a 1 second origin time error, while for an S-P time of 100 seconds, δr is .006, or one part in 130, for an origin time error of 1 second. The required accuracy in r for a specified origin time accuracy increases rapidly with increasing distance.

In practice, a significant portion of the error in determining the S/P travel time ratio results from errors in the S arrival time, either because of difficulty in timing the start of the phase or because of phase misidentification.

If S and P arrival times from several close-in stations are available, Wadati graph analysis (Kisslinger and Engdahl, 1973, Wadati, 1933) may be used to determine the ratio of P to S velocity at the ray bottom and the origin time, if the form of the S-P vs P-O relation and the normal P-O intercept value are known. In the most general case, the Wadati graph is nonlinear and the P-O intercept is not zero. Only if P and S travel times are linear functions of distance is S-P a linear function of P-O; however, the P-O intercept is, in general, still not zero.

In order to derive the relationship let

$$S-T_o = a_s + \Delta/v_s$$

$$P-T_o = a_p + \Delta/v_p$$

Then $$S-P = [a_s - (\rho+1)\, a_p] + \rho\, (P-T_o)$$

where $\rho \equiv v_p/v_s - 1$

or $$S\text{-}P = \rho[P - (T_0 + \tau)] \qquad (2)$$

$$\text{where} \quad \tau = -\frac{1}{\rho}\,[a_S - (\rho + 1)\,a_P]$$

Kaila (1969) and Kaila, Krishna, and Narain (1969) estimated P and S velocities as a function of focal depth for earthquakes in the Hindu-Kush intermediate depth source, using time-distance plots for distances near the inflection point of the time distance curves. Because the ray parameter changes only slowly with distance over this range of distance, the ray parameter may be estimated from the slope of the time-distance curve in this region. Then the velocity at the hypocentral depth can be determined, since the ray corresponding to the inflection point on the travel time curve leaves the hypocenter horizontally (the hypocenter is at the ray bottom for this path) and the depth is presumed known.

In the present study, Wadati graph analysis has been carried out for earthquakes in the Hindu-Kush intermediate depth source, using limited distance ranges to more closely approximate linearity of the Wadati graph, primarily to investigate depth dependence of the P-O intercept. Change of P-O intercept with depth is important because a deviation of the intercept from its expected value, resulting from the difference in actual and initially assumed depths, looks like origin time error when using the S/P technique to locate events of unknown (or uncertain) origin time.

3. EXPERIMENTAL DATA

P and S arrival times from 43 intermediate depth Hindu-Kush calibration earthquakes recorded at 6 WWSSN stations and 19 other close-in stations were used in the study. The calibration earthquakes occurred during 1964 through 1971. All had body wave magnitude of 4.4 or greater and had previously been relocated using preliminary source-region/station time (SRST) corrections (Veith, 1973), and with focal depth restrained to the depth determined from pP-P intervals. Herrin (1968) P travel times were used in making the locations. These locations are considered to be the most reliable locations available for the calibration events. Locations of the calibration earthquakes, both shallow and deep, are shown in figure 1. Table 1 gives the locations and origin times of the calibration earthquakes. Table 2 lists station codes, locations, and elevations of the stations whose data were used in the study. In this table, WWSSN stations are indicated with an asterisk.

P and S times of the events recorded at the six WWSSN stations were reviewed from film reproductions of their seismograms. Arrival times were changed or added when appropriate. P and S arrival times at the other close-in stations were taken from the tri-monthly seismological bulletin of the Moscow Academy of Science and the bulletin of the International Seismological Centre (ISC). In cases where times in Moscow and ISC bulletins disagreed, times were taken from the Moscow bulletin.

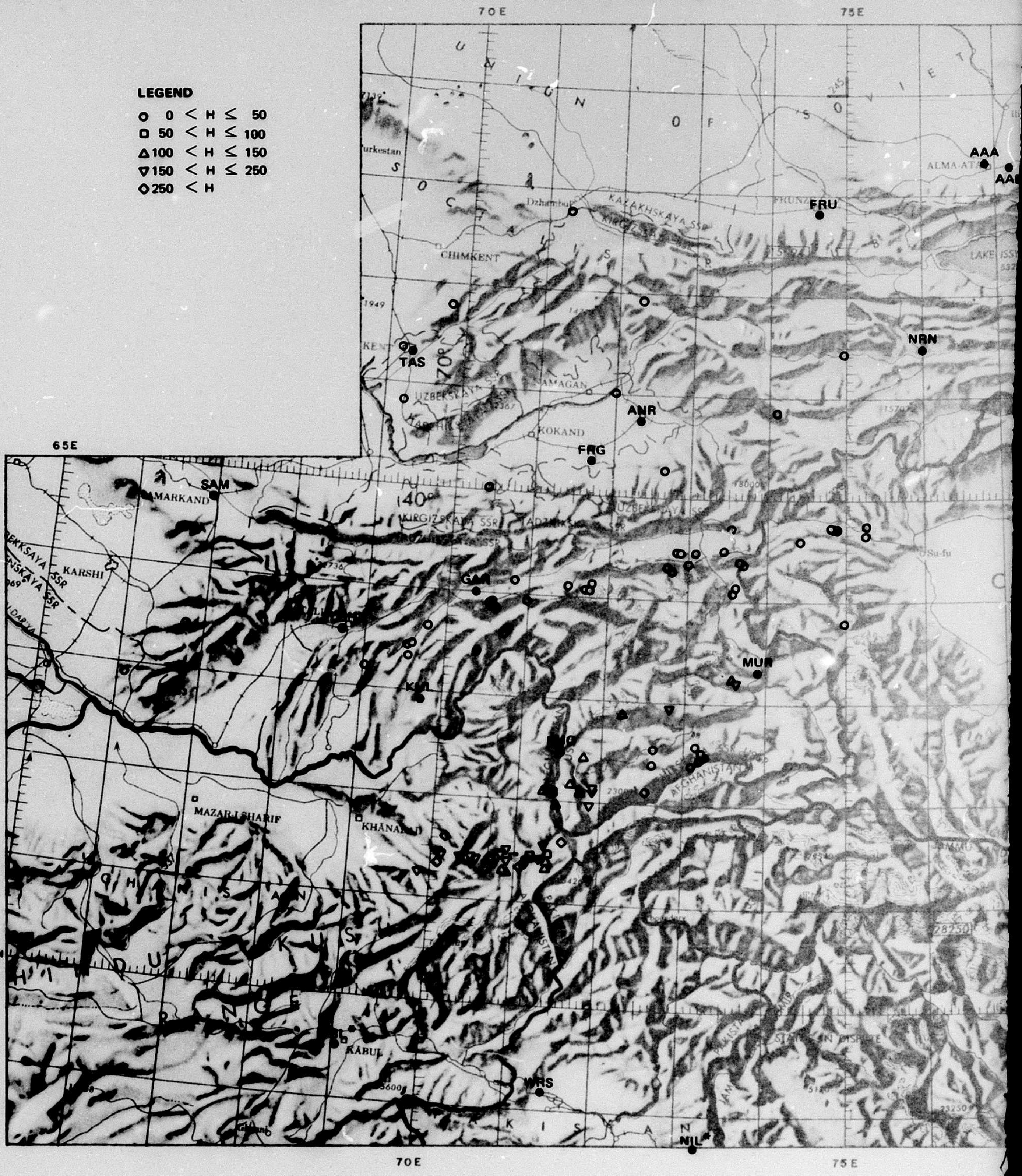
LEGEND
○ 0 < H ≤ 50
□ 50 < H ≤ 100
△ 100 < H ≤ 150
▽ 150 < H ≤ 250
◇ 250 < H
70E
75E
65E
35N
UNION OF SOVIET SOCIALIST REPUBLICS
KAZAKHSKAYA SSR
KIRGIZSKAYA SSR
UZBEKSKAYA SSR
AFGHANISTAN
HINDU KUSH RANGE
Turkestan
Dzhambul
CHIMKENT
ALMA-ATA
FRUNZE
KOKAND
SAMARKAND
KARSHI
MAZAR-I-SHARIF
KHANABAD
KABUL
LAKE ISSYK
AAA
FRU
NRN
TAS
ANR
FRG
SAM
GAR
MUR
WRS
NIL

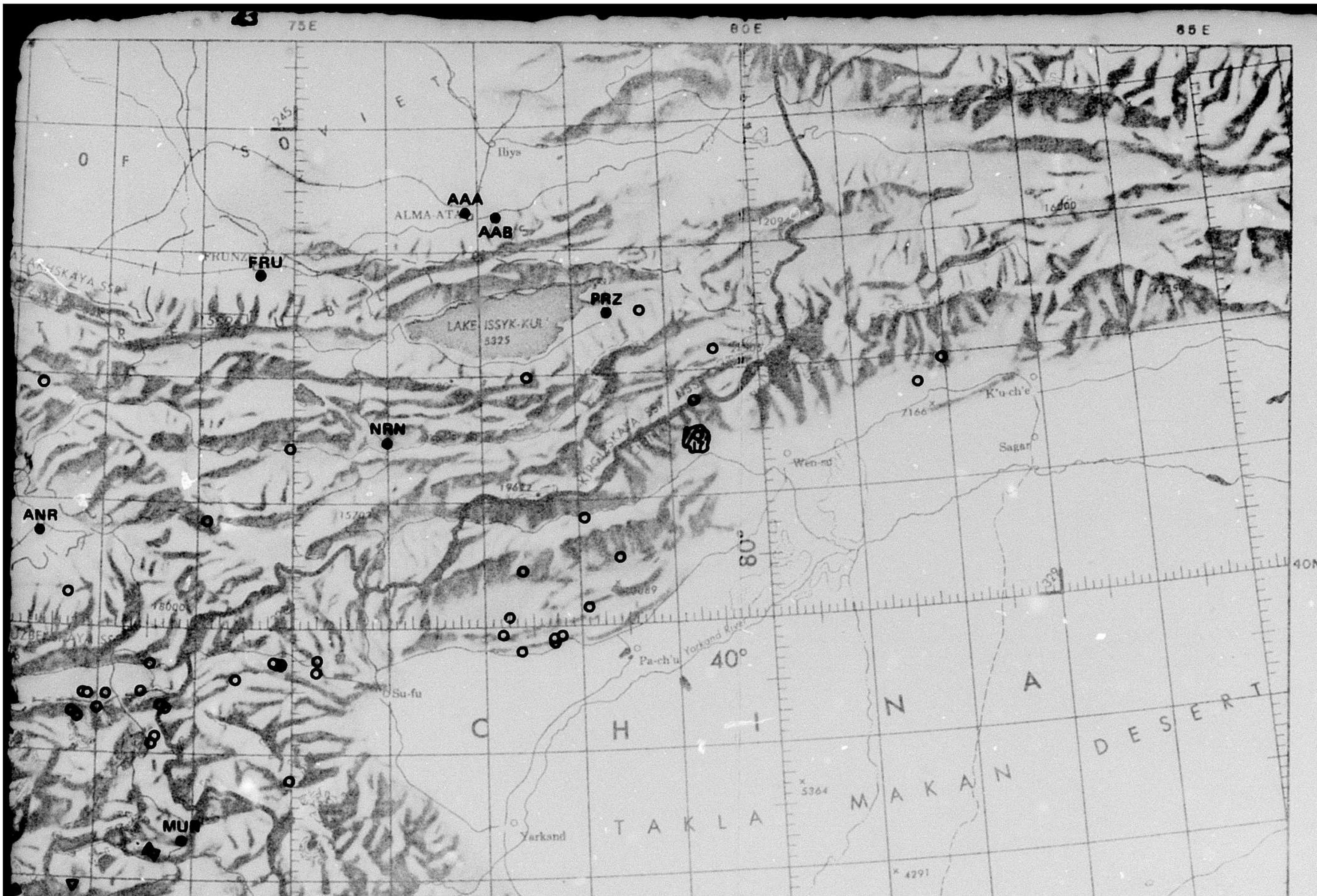

Figure 1. Calibration earthquakes

Table 1. Calibration earthquakes

Date Yr.	Mo.	Da.	Origin Time Hr: Min: Sec:	North Latitude degrees	East Longitude degrees	hpp km	m_b
71	10	14	21:55:55.2	36.51	71.26	86	5.0
67	12	17	00:25:19.2	36.52	71.41	97	5.6
70	09	05	19:26:27.3	37.13	71.42	100	5.0
67	08	12	22:54:39.4	37.11	71.33	101	5.1
71	06	26	22:23:31.4	36.38	71.41	121	5.2
70	11	13	17:30:09.6	36.98	71.50	124	5.1
65	04	10	21:21:29.4	37.44	71.80	124	4.9
68	09	27	10:37:58.9	37.88	72.26	124	5.3
67	11	07	19:57:28.6	37.12	71.77	128	5.0
69	11	24	17:23:23.0	37.19	71.66	129	5.8
70	01	08	21:19:13.7	36.34	70.89	140	4.9
64	12	24	01:08:39.3	36.31	70.94	145	5.2
64	03	23	13:40:31.1	38.25	73.61	150	5.2
64	03	16	03:28:16.2	37.96	72.83	152	5.0
71	03	18	19:12:46.4	38.22	73.64	153	4.9
68	05	08	22:45:10.9	37.17	71.91	161	4.9
71	10	15	16:22:15.3	36.99	71.89	165	4.9
70	12	26	07:58:41.2	36.53	70.91	165	4.4
71	06	22	06:30:03.3	36.29	69.87	167	5.0
64	06	06	08:05:59.8	37.13	71.92	171	4.8
70	06	11	17:40:53.9	36.47	70.99	195	5.1
70	11	29	08:53:25.1	36.58	71.36	200	4.8
69	09	12	05:08:04.3	36.42	70.91	201	4.9
66	08	16	02:16:22.9	36.42	70.79	208	5.5
71	08	04	00:24:39.5	36.40	70.69	210	5.6
65	10	06	15:35:07.2	36.48	70.11	213	5.0
71	08	04	01:59:06.3	36.44	70.73	214	4.9
70	07	21	01:18:08.0	36.46	70.36	215	5.1
66	03	31	23:38:04.3	36.40	70.71	216	5.4
70	09	14	16:11:18.6	36.47	70.14	220	4.8
65	03	14	15:53:09.2	36.38	70.71	220	6.4
64	11	16	04:47:29.9	36.44	70.54	222	5.1
67	05	08	18:48:08.0	36.47	70.13	223	4.8
66	06	06	07:46:18.6	36.39	71.11	225	6.2
70	01	26	16:38:34.1	36.46	70.50	228	4.6
66	06	04	05:11:58.6	36.35	70.69	228	5.4
69	09	04	02:57:22.1	36.51	70.85	231	4.7
69	10	28	18:45:13.5	36.51	70.86	234	5.0
65	07	24	17:57:44.8	36.44	71.15	238	4.7
65	11	16	01:03:58.9	36.38	71.09	252	5.1
65	09	14	18:57:33.1	36.39	70.10	261	4.6
70	09	04	13:12:03.7	36.64	70.17	280	4.7
67	01	25	01:50:22.2	36.63	71.57	289	5.7

Table 2. Station locations

Station	Code	North Latitude deg min sec	East Longitude deg min sec	Elevation meters
Talgar, Kazakh SSR	AAB	43 16 00.0	77 23 00.0	850
Andizhan, Uzbek SSR	ANR	40 45 18.0	72 21 36.0	494
Ashkhabad, Turkmen SSR	ASH	37 57 00.0	58 21 00.0	220
Dehra Dun, India	DD1	30 19 00.0	78 02 00.0	682
Dushambe, Tadzhik SSR	DSH	38 33 30.0	68 46 30.0	817
Fergana, Uzbek SSR	FRG	40 23 00.0	71 47 00.0	600
Frunze, Kirgiz SSR	FRU	42 50 00.0	74 37 00.0	655
Garm, Tadzhik SSR	GAR	39 00 00.0	70 19 00.0	1300
Karachi, Pakistan	KAR	24 56 00.0	67 08 36.0	34
Kizyl-Awat, Turkmen SSR	KAT	39 12 00.0	56 16 00.0	90
Kabul, Afghanistan	KBL*	34 32 27.0	69 02 35.4	1920
Khorog, Tadzhik SSR	KHO	37 29 00.0	71 32 00.0	1850
Kulyab, Tadzhik SSR	KUL	37 54 00.0	69 45 00.0	605
Lahore, Pakistan	LAH*	31 33 00.0	74 20 00.0	210
Mangla, Pakistan	MNL	33 08 50.0	73 45 00.0	436
Meshed, Iran	MSH*	36 18 40.0	59 35 16.0	987
Murgab, Tadzhik SSR	MUR	38 22 00.0	73 56 00.0	3800
New Delhi, India	ND1*	28 41 00.0	77 13 00.0	207
Nilore, Pakistan	NIL*	33 39 00.0	73 15 06.0	536
Naryn, Kirgiz SSR	NRN	41 26 00.0	76 00 00.0	2849
Przhevalsk, Kirgiz SSR	PRZ	42 29 00.0	78 24 00.0	1599
Quetta, Pakistan	QUE*	30 11 18.0	66 57 00.0	1721
Samarkand, Uzbek SSR	SAM	39 40 24.0	66 59 24.0	704
Tashkent, Tadzhik SSR	TAS	41 19 30.0	69 17 42.0	470
Warsak, Pakistan	WRS	34 09 00.0	71 25 00.0	343

*WWSSN Station

4. METHODS

4.1 CALIBRATION OF CLOSE-IN STATIONS

For each calibration earthquake, values of the S/P travel time ratio r (see equation 1) were computed from

$$r = (S-P)/(P-T_{pP}) \qquad (3)$$

where T_{pP} ≡ origin time estimate from relocation restrained to pP depth for each station that recorded both P and S from the event. Mean values of r were computed using the station mean r values by

$$\delta T_{1ij} = (P-T_{pP})_{ij} - (S-P)_{ij}/\bar{r}_i \tag{4}$$

where $\bar{r}_i \equiv$ mean r for station $\underline{i}$

$\delta T_{1ij} \equiv$ origin time deviation for station $\underline{i}$ and event $\underline{j}$.

Station and event origin time deviations (S_{1i} and E_{1j}, respectively) were computed using the station mean r values from

$$S_{1i} = \frac{1}{n_i} \sum_{j=1}^{n_i} \delta T_{1ij} \tag{5}$$

where n_i = number of events for which station $\underline{i}$ had data

$$E_{1j} = \frac{1}{n_j} \sum_{i=1}^{n_j} \delta T_{1ij} \tag{6}$$

where $n_j \equiv$ number of stations with data for event $\underline{j}$

In addition, station and event origin time deviations (S_{2i} and E_{2j}, respectively) were computed using the same value of r (the overall mean value) for all stations:

$$S_{2i} = \frac{1}{n_i} \sum_{j=1}^{n_i} [(P-T_{pP})_{ij} - (S-P)_{ij}/\bar{r}\,] \tag{7}$$

$$E_{2j} = \frac{1}{n_j} \sum_{i=1}^{n_j} [(P-T_{pP})_{ij} - (S-P)_{ij}/\bar{r}\,] \tag{8}$$

where $\bar{r} \equiv$ overall mean r

Results are given in section 5.3.

4.2 WADATI GRAPH ANALYSIS

To investigate the sensitivity of the S/P travel time ratio to changes in focal depth, Wadati graph analysis was performed on the data for each event, using only arrivals within a restricted distance range. Based on the results reported by Kaila, and others (1969) on S and P travel times from Hindu-Kush earthquakes, a distance range of 4.5 to 13.0 degrees was selected, to assure that the assumption of a linear relation between S-P and P-O is justified. Reliable estimates of Wadati graph parameters could not be obtained for individual events because too few stations within the restricted distance range recorded both P and S for any single event. Therefore, data from earthquakes of similar depth were combined and least squares estimates of the Wadati graph slope (ρ) and P-O intercept (τ) were determined for each of 10 depth ranges. This procedure is valid if the pP origin times are correct and if the Wadati graph parameters do not change rapidly with depth.

The Wadati graph for intermediate depth earthquakes should not be linear at distances less than about 4.5 degrees. However, because almost half the data fall in this distance range, it is of interest to determine if S and P arrival times at stations in this distance range can be used to compute accurate origin times, using the slope and P-O intercept determined from Wadati graph analysis. Wadati graph analysis should also aid in investigating sensitivity of the S/P travel time ratio to changes in focal depth and epicentral distance over this distance range. Therefore, linear Wadati graph parameters were estimated for each of the 10 depth ranges, using only arrivals at distances less than 4.5 degrees.

Using the weighted mean values of Wadati graph slope ($\bar{\rho}$) and P-O intercept ($\bar{\tau}$), origin time deviations from the pP values were computed by

$$\delta T_{3ij} = (P-T_{pP})_{ij} - \bar{\tau}_k - (S-P)_{ij}/\bar{\rho}_k \qquad (9)$$

where k ≡ distance range index

Mean station (S_{3i}) and event (E_{3j}) origin time deviations were computed by taking the appropriate mean of the deviations defined by equation (9). The event origin time deviations were computed for each distance range separately and for the two distance ranges combined. Then residual event origin time deviations were computed by

$$E_{4j} = E_{3j} - \frac{1}{n_j} \sum_{i=1}^{n_j} S_{3i} \qquad (10)$$

where n_j ≡ number of stations with data for event j.

Results are given in section 5.3.

5. RESULTS AND DISCUSSION

5.1 DEPTH DEPENDENCE OF P/S VELOCITY RATIO

Table 3 lists the Wadati graph parameters estimated from the data grouped by depth range for the two distance ranges, 4.5 to 13.0 degrees and less than 4.5 degrees. Figure 2 shows the Wadati graph slopes and P-T_{pp} intercepts, with plus or minus one standard error limits, as a function of pP depth for the distance range 4.5-13.0 degrees, with the mean slope and intercept indicated. Also shown on this figure are values of Wadati graph slope (ρ) and P-O intercept (τ) computed from the P and S velocity values reported by Kaila, et al (1969) for the Hindu-Kush region and smooth curves of ρ and τ (see equation 2) as functions of hpP computed from Kaila's linear velocity-depth functions. Most of the difference between Kaila's intercept values and the intercept values determined in the present study can be accounted for by the different P travel times used, Jeffreys-Bullen (1958) (JB) in Kaila's study and Herrin (1968) in the present study. Locations made with Herrin times yield origin times about 2.5 seconds later, on the average, than locations made with JB times.

The minima in the P to S velocity ratio (ρ+1) and P-O intercept in the 140 to 170 km depth ranges appear to be real. However, in view of the error limits on slope and intercept estimates for the individual depth ranges, constant slope and intercept values over the full depth range constitute a plausible interpretation of the data. Deviations of the intercept values from the overall mean value (+ 1.6 second) range from +2.1 to -1.9 seconds. If interpreted as origin time errors, and assuming a mean depth derivative of about -0.1 second/km for events in this depth range, corresponding depth errors would be about ±20 km.

Wadati graph parameters as a function of pP depth for distances less than 4.5 degrees, with the mean slope and intercept indicated, are shown in figure 3. For this distance range, rays do not leave the focus horizontally. Therefore, the Wadati graph slope can not be interpreted in terms of the ratio of P to S velocity at the hypocentral depth. However, the technique provides a means of using data from stations in this distance range to compute origin times from P and S arrival times, recognizing that the assumption of a linear Wadati graph is only approximate in this case.

5.2 DISTANCE AND DEPTH DEPENDENCE OF THE S/P TRAVEL TIME RATIO

Figures 4 through 8 show observed values of r (= (S-P)/(P-TpP)) as a function of P-T_{pP} for each of the 10 depth ranges used in the Wadati graph analysis. The smooth curves shown on each figure represent the expected value of r, computed from the mean Wadati graph parameters for the two distance ranges.

The large increase in observed r values at very close distances is accounted for by the strong negative P-O intercept for the Wadati graph for this distance range (figure 3). For distances greater than 4.5 degrees, distance dependency of the S/P travel time ratio is no strong, the slight increase in r with increasing distance being accounted for by the positive Wadati graph intercept for this distance range (figure 2). The strongest evidence of depth dependency

Table 3. Wadati graph parameters, by depth

Depth (km)	86-101	121-129	140-153	161-171	195-201	208-216	220-2[illegible]	228-238	252-261	280-289
No. events	4	6	5	5	3	6	5	5	2	2

Epicentral Distance <4.5°

Mean depth(km)	95	125	149	165	198	213	222	232	256	282
No. obser.	20	29	23	28	11	29	20	28	13	8
$\hat{\rho}$	.724	.694	.701	.683	.763	.704	.778	.734	.716	.746
stnd err ρ	.032	.024	.027	.024	.055	.024	.024	.017	.033	.032
$\hat{\tau}$ (sec)	-2.43	-5.22	-5.30	-5.20	-0.45	-3.96	+0.35	-2.46	-5.11	-1.12
stnd err τ	1.64	1.07	1.25	1.19	2.67	1.19	1.17	0.85	1.59	1.75

$\bar{\rho}$ = 0.713

$\bar{\tau}$ = -3.72

Epicentral Distance 4.5° - 13.0°

Mean depth(km)	98	125	146	165	198	213	222	231	257	284
No. obser.	19	34	27	26	15	52	22	34	13	17
$\hat{\rho}$	.795	.802	.781	.769	.807	.792	.780	.787	.793	.805
stnd err ρ	.015	.012	.014	.013	.023	.012	.015	.012	.021	.018
$\hat{\tau}$ (sec)	+2.56	+2.82	+0.09	-0.26	+3.76	+2.12	+0.81	+0.72	+0.64	+3.33
stnd err τ	1.64	1.43	1.72	1.56	2.63	1.39	1.66	1.44	2.20	2.07

$\bar{\rho}$ = 0.790

$\bar{\tau}$ = +1.63

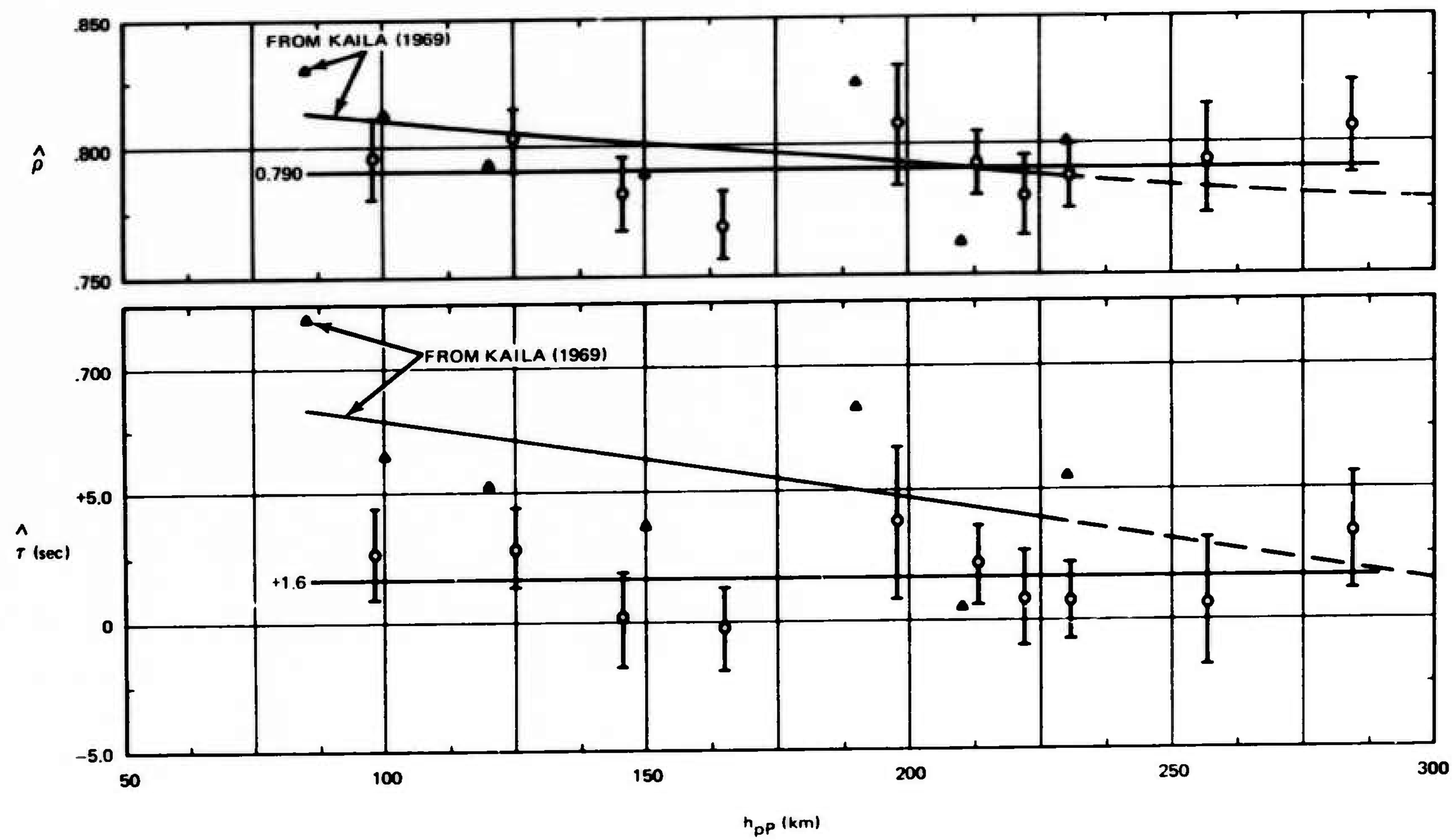

Figure 2. Wadati graph parameters for distances range 4.5 to 13.0 degrees

G 7708

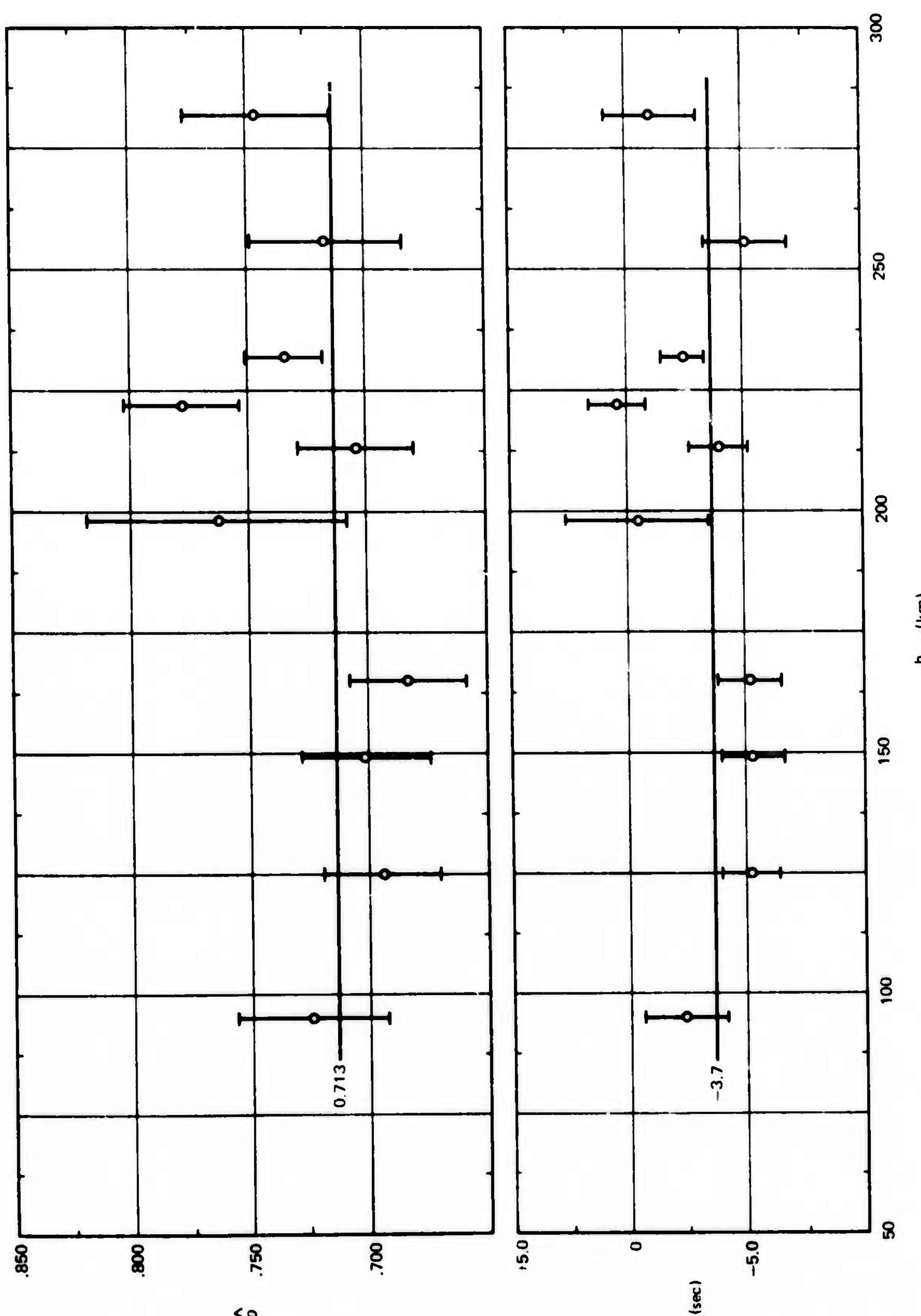

G 7709

Figure 3. Wadati graph parameters for distances less than 4.5 degrees

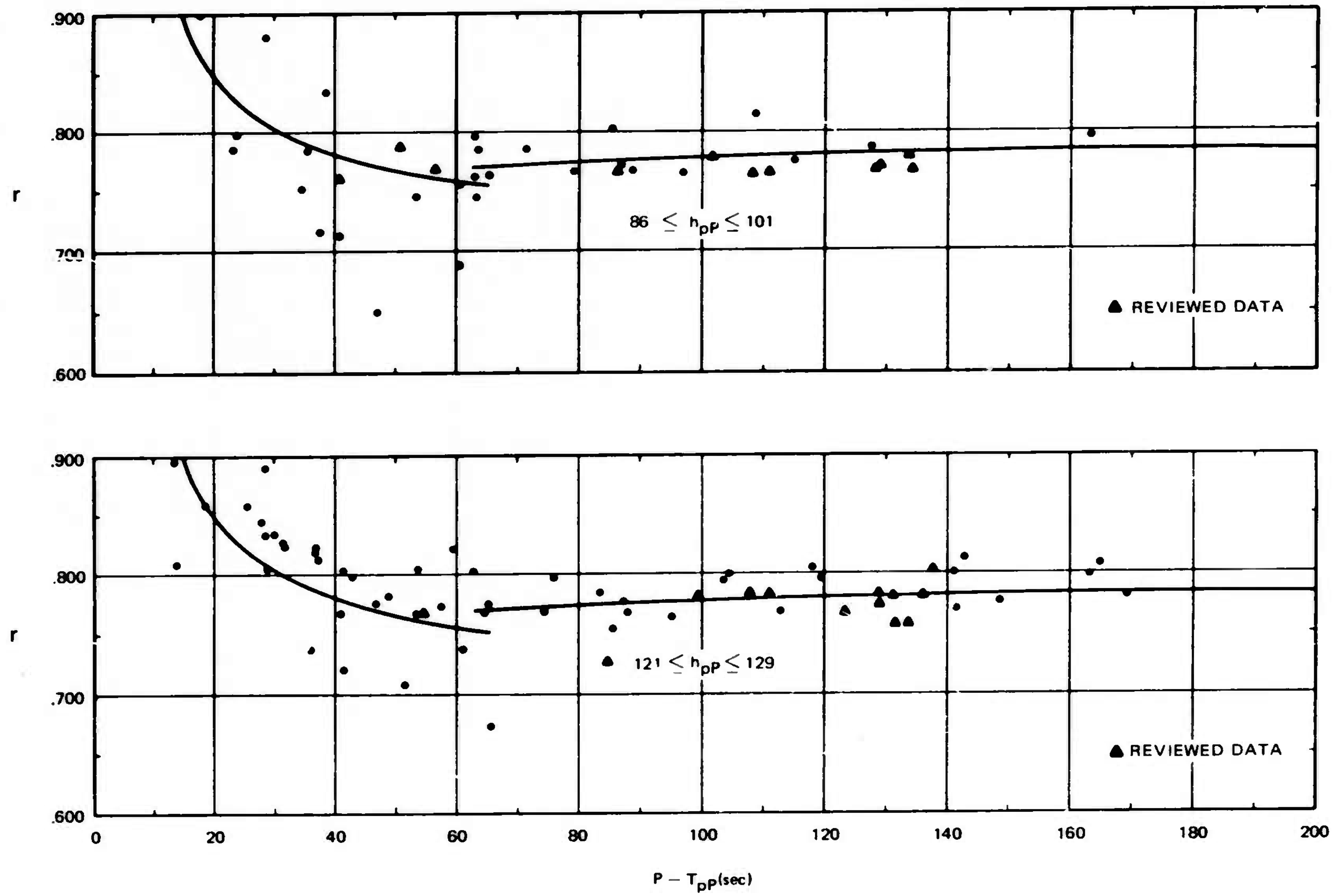

Figure 4. S/P travel-time ratio for depth ranges 86-101 km and 121-129 km

G 7710

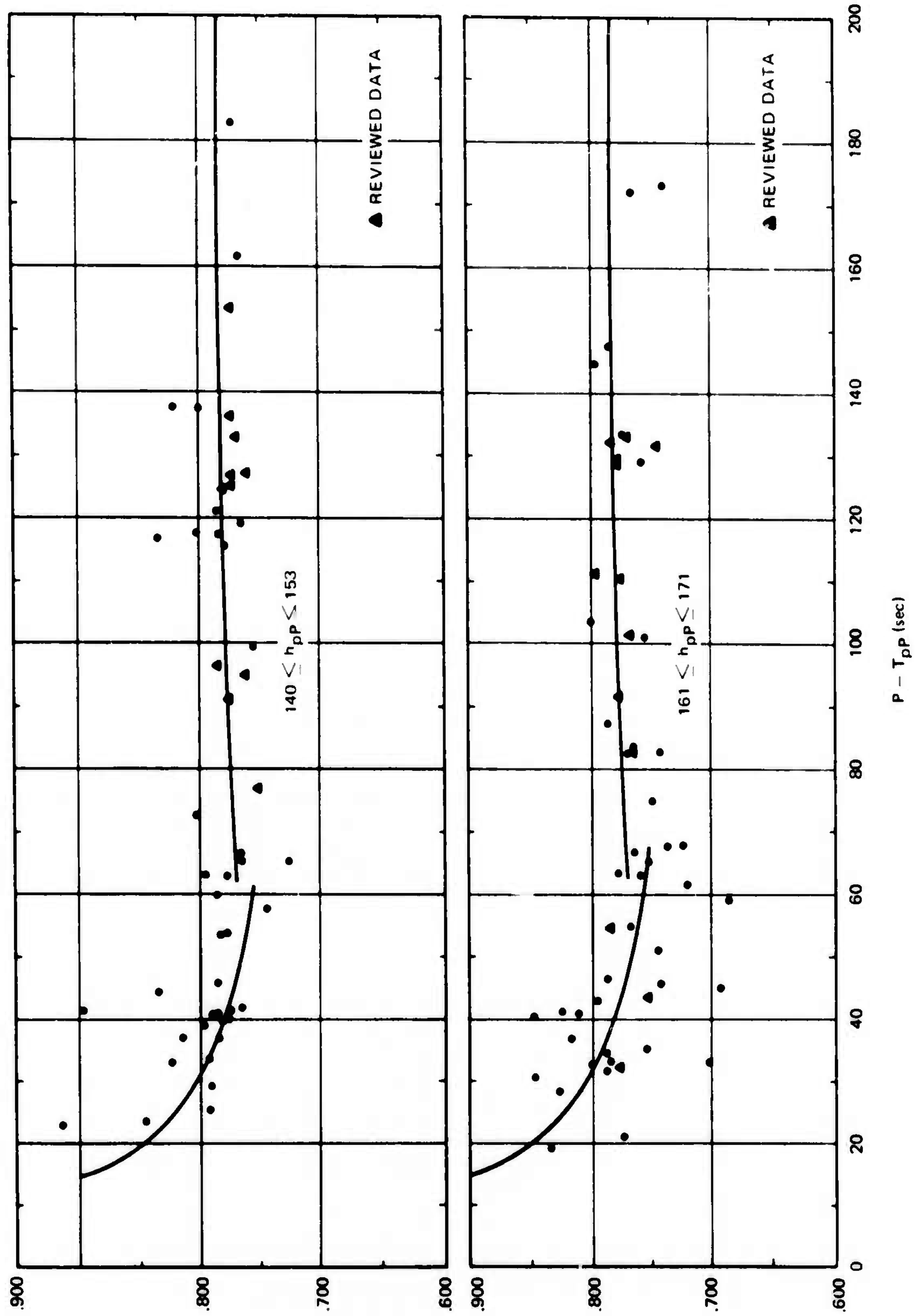

G 7711

Figure 5. S/P travel-time ratio for depth ranges 140-153 km and 161-171 km

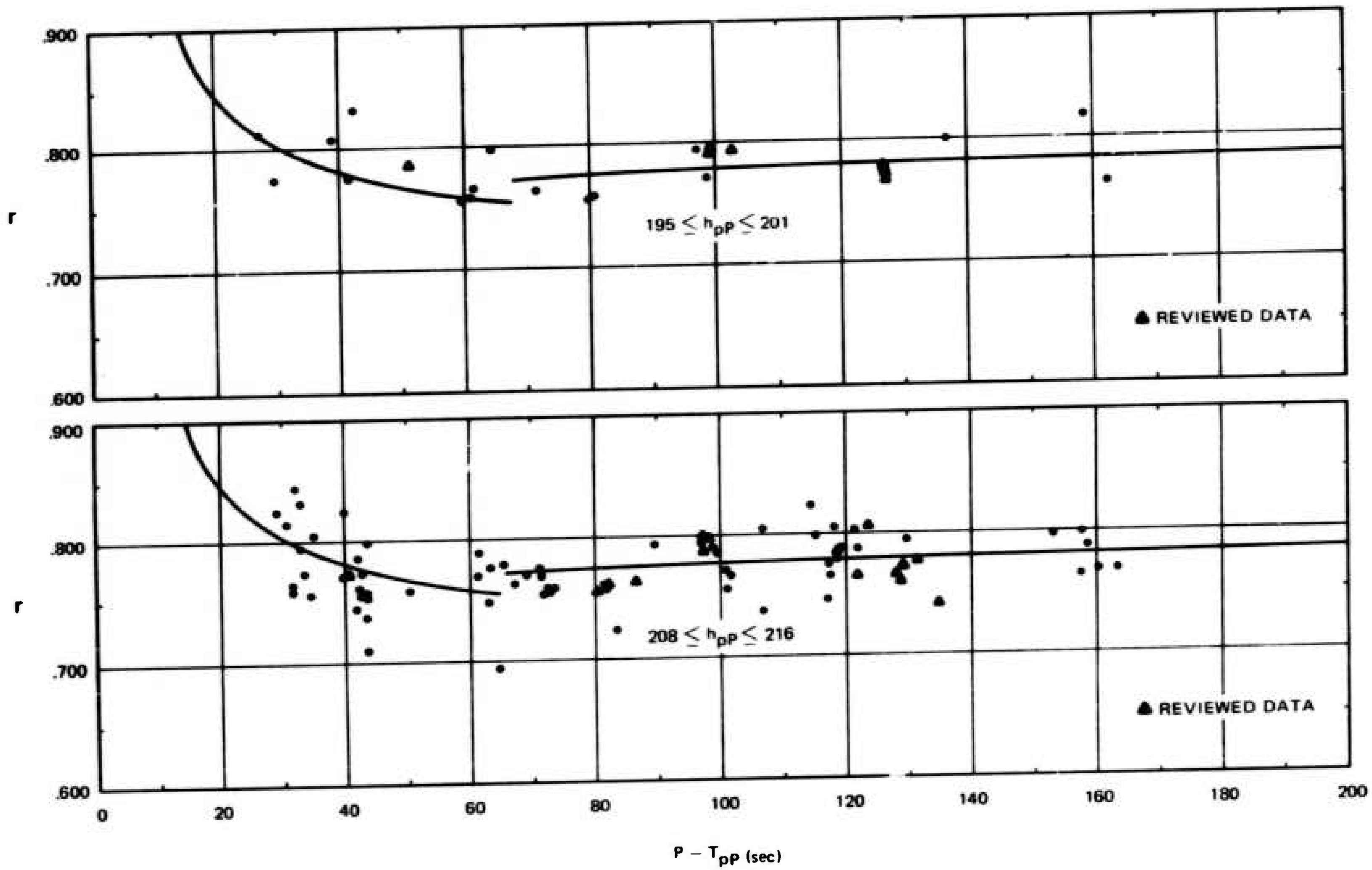

Figure 6. S/P travel-time ratio for depth ranges 195-201 km and 208-216 km

G 7712

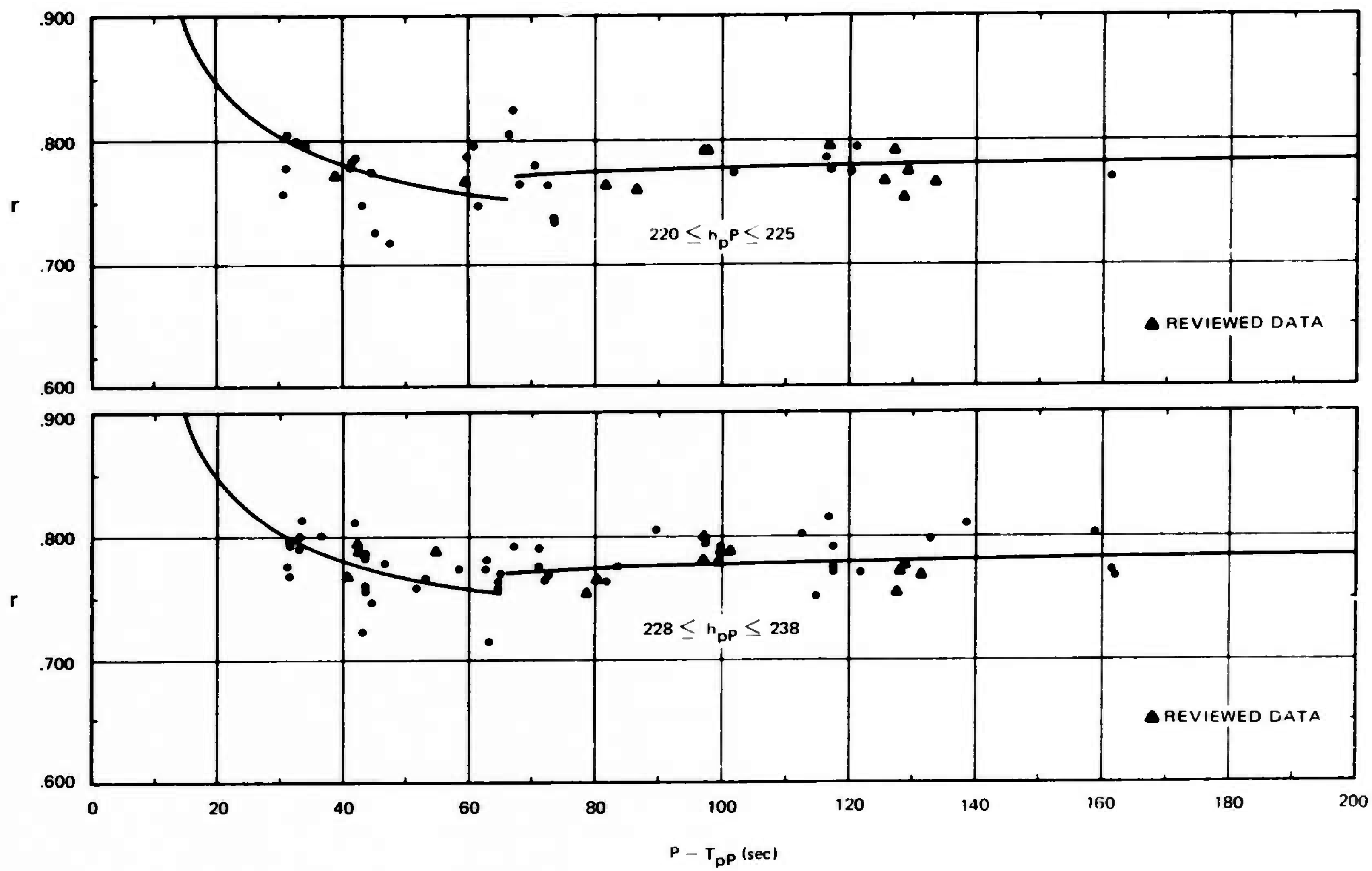

Figure 7. S/P travel-time ratio for depth ranges 220-225 and 228-238 km

G 7713

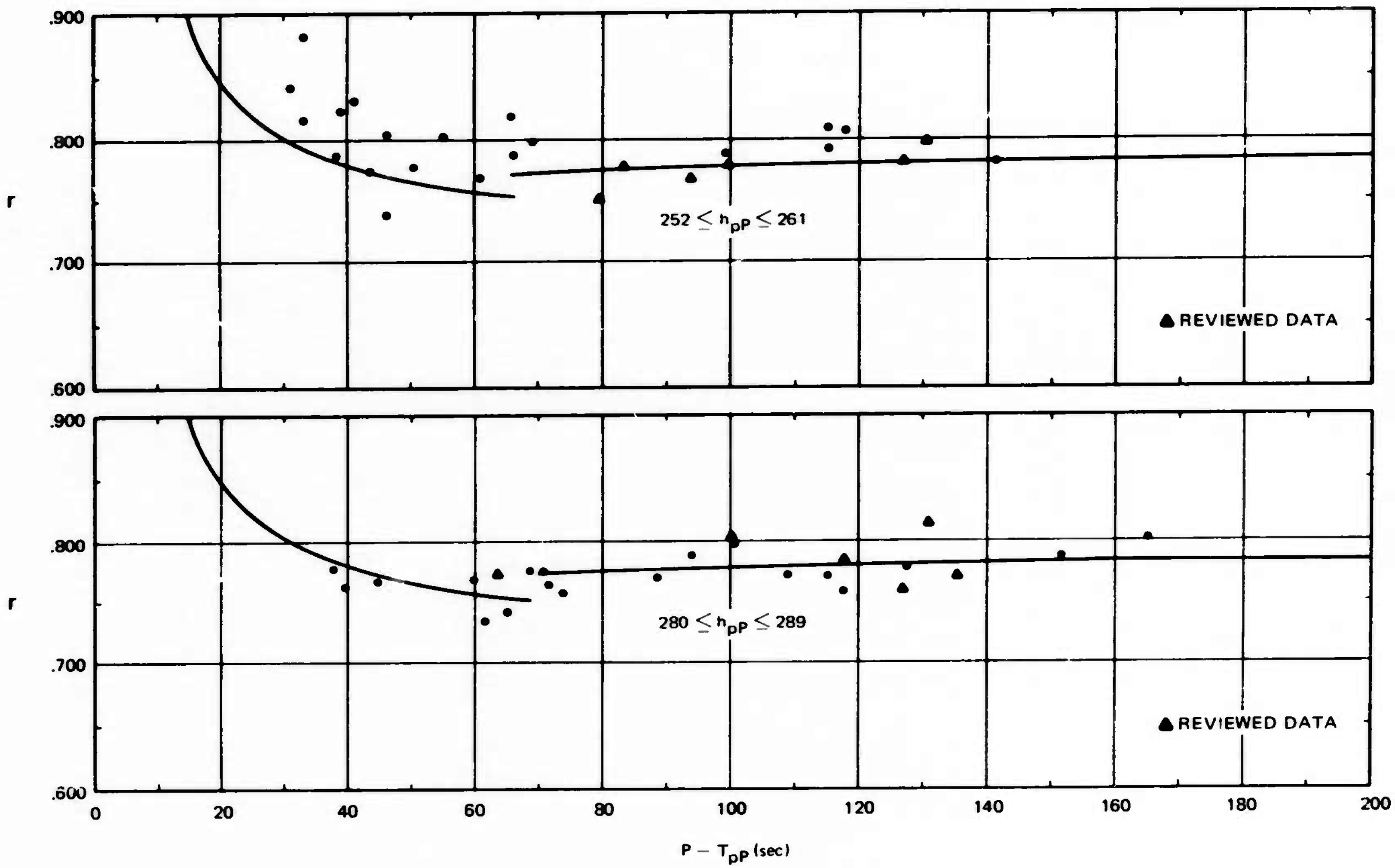

Figure 8. S/P travel-time ratio for depth ranges 252-261 and 280-289 km

G 7714

of r occurs for the 161 to 171 km depth range, for which the curve computed from the mean Wadati graph parameters gives r values mostly larger than observed values and the 252 to 261 km depth range, for which the r values computed from the mean Wadati graph parameters are smaller than observed values (see also figures 2 and 3). In general as expected from results of the Wadati graph analysis (figures 2 and 3), the curves computed from the mean Wadati graph parameters represent the observed S/P travel time ratios better for the 4.5 to 13 degree distance range than for the less than 4.5 degree range.

5.3 S/P ORIGIN TIME ESTIMATES

Principal results of the study to date are summarized in table 4, giving station statistics and table 5, giving statistics on estimates of event origin time deviations, using the different techniques described in section 4.

Table 4 lists the mean r and standard deviation of r for each station, the mean and standard deviation of origin time deviations from the pP value using the station mean r for all events (S_{1i}), using the same value (0.780) of r for all stations (S_{2i}), and using the mean Wadati graph parameters (S_{3i}). Table 5 summarizes event origin time deviations from the pP value computed with the various techniques: using the station mean r's (E_{1j}, equation 6) both using all stations and using only stations whose data were reviewed (with the requirement that at least two stations have data for each event), using the same value of r (0.780) for all stations (E_{2j}, equation 8), and using the mean Wadati graph slope and intercept for the appropriate distance range, for the two distance ranges both separately and combined. In addition, the residual event origin time deviations (E_{4j}, equation 10), after removing the station mean P-O intercepts (S_{3i}) are included in table 5.

Figure 9 shows the event origin time deviations, computed by the different techniques, as a function of pP depth. No clear trend with depth is apparent for origin time deviations computed by any of the four techniques, indicating that, for identification purposes, depth dependency of the S/P travel time ratio or the Wadati graph parameters is not serious for this region. Locations of the two earthquakes with the largest residual origin time deviations (E_{j4}:+2.5 seconds at 165 km and -2.2 seconds at 261 km) were based on pP depths less well determined than those of the other calibration earthquakes; therefore, errors in the calibration depths may account for these large deviations.

As is evident from the results shown in table 5, there was little difference in origin time deviations from the pP values computed by the different techniques based on S/P travel time ratios. Using each station's mean r (E_{1j}) did as well as using the estimates of slope ($\rho = v_p/v_s - 1$) and intercept (τ) from the Wadati graph analysis (E_{3j}) with the two distance ranges combined, both techniques giving a standard deviation of origin time deviation of 0.9 second. For events in the intermediate depth range, the corresponding depth error (deviation from pP depth) would have a standard deviation of 8-9 km.

Removing the mean station effect (S_{3i}) resulted in a further slight reduction in standard deviation of origin time deviation from the pP value (E_{4j} in table 5). Because of the large values of the mean station effects for some stations (S_{3i} in table 4), it is important to correct for these factors when using only a few stations to compute origin times by means of the Wadati graph parameters.

Table 4. Station S/P travel time ratios and origin time deviations

Station	No. of events	Mean dist. (deg)	r mean	r St dv	secs S_{1i} mean	secs S_{1i} St dv.	secs S_{2i} mean	secs S_{2i} st dv	secs S_{3i} mean	secs S_{3i} st dv
KHO	32	1.18	.807	.047	0.2	1.5	-0.8	1.5	0.2	1.5
KUL	22	1.75	.813	.037	0.2	1.4	-1.3	1.5	-0.6	1.6
KBL*	9	2.32	.772	.013	0.0	0.7	0.4	0.7	0.4	0.8
GAR	28	2.50	.780	.051	0.2	2.6	0.1	2.6	0.2	2.7
MUR	7	2.73	.778	.029	0.1	1.5	0.2	1.5	-0.2	1.7
DSH	36	2.74	.778	.038	0.0	2.0	0.2	2.0	0.0	2.1
WRS	11	2.93	.758	.045	0.2	2.8	1.5	2.8	0.9	2.8
FRG	9	3.56	.782	.020	0.2	1.3	0.0	1.3	-1.2	1.1
NIL*	8	3.58	.778	.010	0.1	0.7	0.2	0.7	-1.3	0.6
ANR	29	4.05	.773	.025	0.0	1.9	0.5	1.9	-0.8	2.0
MNL	13	4.14	.758	.032	0.0	2.7	1.8	2.7	-0.2	2.9
SAM	12	4.38	.737	.036	-0.1	3.1	3.5	2.9	2.0	2.8
TAS	33	4.84	.771	.020	0.1	1.7	0.9	1.8	0.0	1.9
LAH*	26	5.89	.760	.014	0.0	1.6	2.1	1.5	1.5	1.5
NRN	5	6.04	.792	.015	-0.1	1.6	-1.4	1.7	-1.9	1.6
FRU	27	6.71	.776	.015	-0.1	1.8	0.4	1.8	0.0	1.8
QUE*	30	7.35	.784	.011	0.0	1.4	-0.5	1.4	-0.8	1.5
PRZ	15	8.36	.792	.014	0.0	2.0	-1.8	2.0	-1.9	2.0
AAB	13	8.49	.785	.031	0.0	4.6	-0.8	4.7	-0.9	4.6
DDI	15	8.58	.781	.013	0.0	1.8	-0.2	1.9	-0.3	1.9
MSH*	20	9.45	.783	.013	0.0	2.1	-0.5	2.1	-0.5	2.1

* WWSSN station - data reviewed

Table 4 (Continued)

Station	No. of events	Mean dist. (deg)	r mean	r St dv	secs S_{1i} mean	S_{1i} St dv	secs S_{2i} mean	S_{2i} St dv	secs S_{3i} mean	S_{3i} St dv
NDI*	33	9.55	.767	.011	0.1	1.8	2.1	1.8	2.1	1.8
ASH	12	10.33	.797	.015	0.1	2.7	-2.9	2.7	-2.7	2.7
KAT	13	12.02	.789	.016	-0.1	3.4	-1.9	3.4	-1.5	3.4
KAR	10	12.08	.771	.017	0.1	3.7	2.0	3.7	2.4	3.6

*WWSSN station - data reviewed

Table 5. Event origin time deviations

Event origin time deviation	P-O intercept	Slope	Station correction		Mean secs	St dv secs
E_{1j}	0	$\bar{r}_i$	0	All stas	-0.01	0.86
				reviewed stas and 2 or more	+0.03	1.07
E_{2j}	0	$\bar{r}$	0	All stas	+0.25	0.95
				reviewed stas and 2 or more	+0.61	1.17
E_{3j}	$\bar{\tau}_k$	$\bar{\rho}_k$	0	both Δ ranges	-0.03	0.90
				$\Delta < 4.5°$	-0.09	1.08
				$4.5° \leq \Delta \leq 13.0°$	+0.02	1.09
E_{4j}	$\bar{\tau}_k$	$\bar{\rho}_k$	S_{3i}	both Δ ranges	0.00	0.84
				$\Delta < 4.5°$	-0.10	1.20
				$4.5° \leq \Delta \leq 13.0°$	-0.01	0.93

i : station index

j : event index

k : distance range index

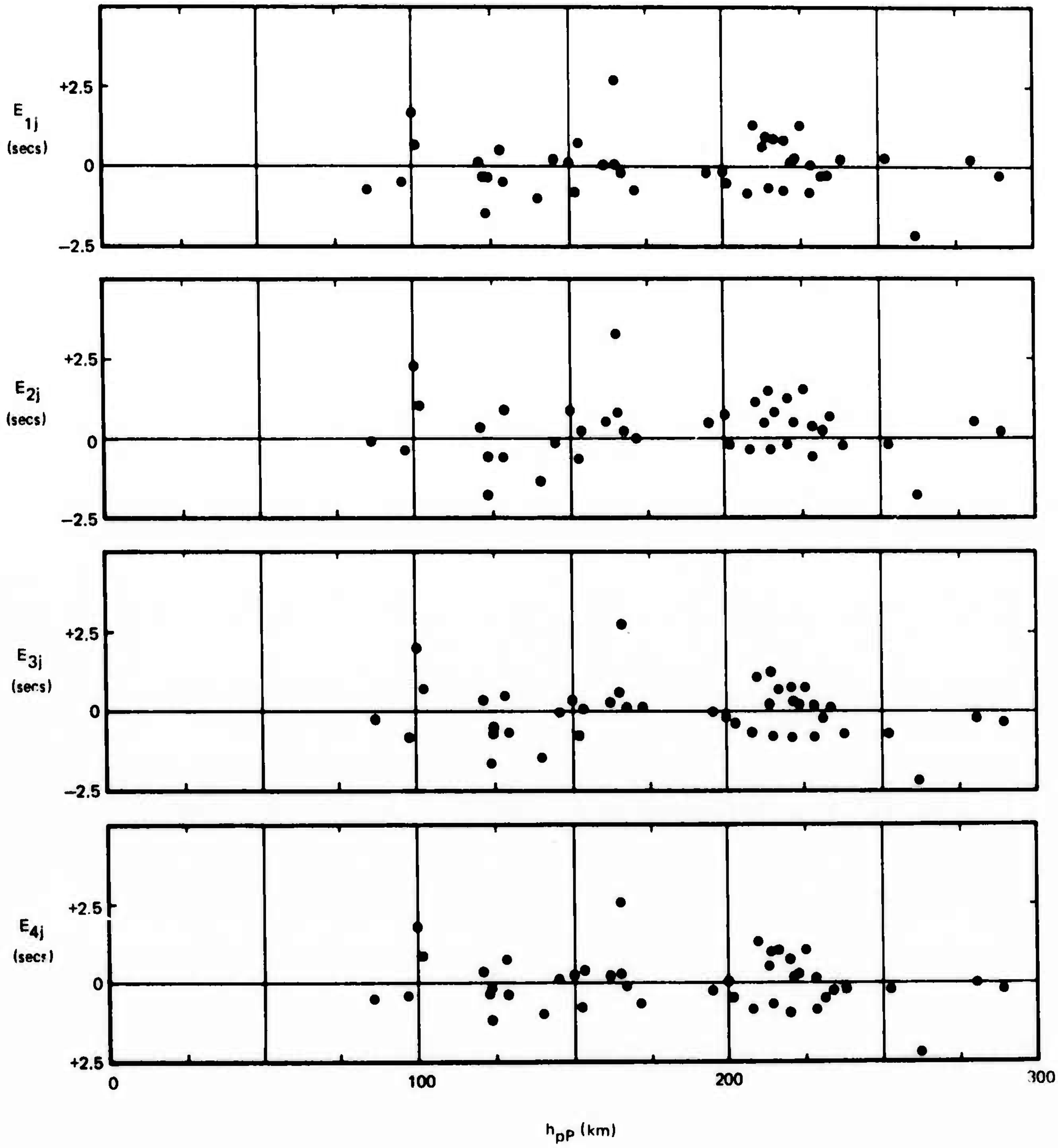

Figure 9. Origin time deviations from T_{pP}

G 7715

For identification purposes, using the same value of r for all stations (E_{2j}) is entirely adequate for Hindu-Kush intermediate depth earthquakes, the standard deviation of origin time deviations for this case being 1.0 second, with a corresponding standard deviation of depth error of about 10-12 km.

6. CONCLUSIONS AND RECOMMENDATIONS

The S/P travel time ratio technique of computing focal depth will identify Hindu-Kush intermediate depth earthquakes if reliable S and P arrival times at stations within 13 degrees of the epicenter are available. Variation of the S/P travel time ratio with epicentral distance is not significant for the distance range 4.5 to 13 degrees. For distances less than 4.5 degrees, the S/P travel time ratio increases rapidly with decreasing distance. For the Hindu-Kush intermediate depth source, depth dependence of the S/P travel time ratio is weak and can be neglected for identification purposes.

We recommend that the investigation of the S/P travel time ratio in Central Asia be continued. Close-in stations should be calibrated for the S/P travel time ratio for shallow earthquakes in this region. Sensitivity of the observed travel time ratio to changes in focal depth should be investigated. The depth accuracy obtainable for shallow Central Asia earthquakes should be determined.

7. REFERENCES

Evernden, J. F., 1969, Identification of earthquakes and explosions by use of teleseismic data: J. Geophys. Res., v. 74, no. 15, p. 3828-3856.

Herrin, E., ed., 1968, Seismological tables for P: Bul. Seism. Soc. Amer., v. 58, no. 4, p. 1196-1220.

Jeffreys, H. and Bullen, K. E., 1958, Seismological tables: London, British Assoc. for the Advancement of Science, Gray Milne Trust, 50 p.

Kaila, K. L. 1969, A new analytical method for finding the upper mantle velocity structure from P and S wave travel times of deep earthquakes: Bul. Seism. Soc. Amer., v. 59, no. 2, p. 755-769.

Kaila, K. L., Krishna, V. G., and Narain, H., 1969, Upper mantle velocity structure in the Hindu-Kush region from travel time studies of deep earthquakes using a new analytical method: Bul. Seism. Soc. Amer., v. 59, no. 5, p. 1949-1967.

Kisslinger, C. and Engdahl, E. R., 1973, The interpretation of the Wadati diagram with relaxed assumptions: Bul. Seism. Soc. Amer., v. 63, no. 5, p. 1723-1736.

Macelwane, J. B. and Sohon, F. W., 1932, Introduction to theoretical seismology: Part I, Saint Louis, Mo., St. Louis University.

Swanson, J. G., 1969, Estimation of focal depth from close-in P and S data (U): TR 69-34, Garland, Texas, Geotech, a Teledyne Co., 30 p.

______________, 1971, P-to-S velocity ratio in Central Asia (U): TR 71-14, Garland, Texas, Teledyne Geotech, 25 p.

Veith, K. F. and van Leer, F. P., 1970, Hypocenter determination methods and control: TR 70-20, Garland, Texas, Teledyne Geotech, 30 p.

Veith, K. F., 1973, Progress report on hypocenter refinement in Central Asia (U): TR 73-9, Garland, Texas, Teledyne Geotech, 37 p.

Wadati, K., 1933, On the travel time of earthquake waves: Part II, Geophys. Mag., v. 7, p. 101-111.